Atomic geometry of Ge(111) $\sqrt{3} \times \sqrt{3}R\,30°$-Ag determined by low-energy electron diffraction

H. Huang, H. Over,* and S. Y. Tong

Department of Physics and Laboratory for Surface Studies, University of Wisconsin—Milwaukee,
P.O. Box 413, Milwaukee, Wisconsin 53201

J. Quinn and F. Jona

Department of Materials Science and Engineering, State University of New York, Stony Brook, Stony Brook, New York 11794-2275
(Received 1 December 1993)

We have carried out a quantitative low-energy electron-diffraction intensity analysis of the Ge(111) $\sqrt{3} \times \sqrt{3}R\,30°$-Ag structure. It is found that the Ag atoms arrange according to a honeycomb chained trimer model (HCT) similar to the situation of Si(111) $\sqrt{3} \times \sqrt{3}R\,30°$-Ag. This result shows that the Ge-Ge bond is stronger than the Ag-Ag bond on the surface, thus causing the HCT structure to form.

The atomic structure and bonding of noble-metal atoms like Ag and Au on semiconductor (Si,Ge) surfaces have been studied extensively over the past 30 years to obtain general insight into the formation of the metal-semiconductor interface. In particular, it is important to determine the relative strengths of the metal-metal and semiconductor-semiconductor bonds at the interface. On the (111) surface of Si and Ge, both Ag and Au adsorption induce a surface $\sqrt{3} \times \sqrt{3}R\,30°$ reconstruction.[1] For the Si(111) $\sqrt{3} \times \sqrt{3}R\,30°$-Ag surface, the structure from most works[2-10] is an arrangement in which the Ag atoms substitute the first-layer Si atoms in positions slightly displaced from bulk sites (missing top layer), while the remaining Si atoms in the topmost double layer form trimers (see Fig. 1). The corresponding scanning tunneling microscope (STM) image of empty states shows a honeycomb pattern[11-13] (two bright spots per $\sqrt{3} \times \sqrt{3}$ unit cell). The STM image is consistent with the electronic density of an empty surface band near the Fermi level rather than with the atomic positions of the Ag atoms.[6] This model is generally called the honeycomb-chained-trimer (HCT) model.

With Si(111) $\sqrt{3} \times \sqrt{3}R\,30°$-Au, experimental and theoretical studies point toward a different model. STM observations[14-15] reveal an image with only one bright spot in each $\sqrt{3} \times \sqrt{3}$ unit cell. Detailed studies by different techniques[16-20] show clear evidence for a missing top layer model. However, the Si atoms do not form trimers; instead, Au atoms in the top layer are trimerized centered over T_4 sites (fourth-layer atoms). This model is referred to as the conjugate HCT model (CHCT).[19] A similar structure has also been found for Ge(111) $\sqrt{3} \times \sqrt{3}R\,30°$-Au, using x-ray diffraction (XRD) analysis.[21] The reasons for HCT and CHCT formation at the interface are attributed to the relative strengths of the metal-metal and semiconductor-semiconductor bonds, as explained by Ding, Chan, and Ho.[19]

In this paper we report dynamical low-energy electron-diffraction (LEED) analysis of the Ge(111) $\sqrt{3} \times \sqrt{3}R\,30°$-Ag interface. The results show that the HCT model is favored over the CHCT model. The stronger Ge-Ge bond results in Ge trimerization and this

greatly distorts the Ge lattice, so that large relaxations were found down to the sixth atomic layer. Our result is corroborated by a photoelectron spectroscopic study which shows that the electronic properties of $\sqrt{3} \times \sqrt{3}R\,30°$-Ag on Si(111) and Ge(111) are very much the same.[1,22] Also, the growth modes with substrates at room and elevated temperatures are similar for both systems,[1] and the $\sqrt{3} \times \sqrt{3}R\,30°$ LEED pattern is formed only at elevated temperatures. Our result differs from that of an XRD study, which preferred the CHCT model because of striking similarities in the Patterson functions of Ge(111) $\sqrt{3} \times \sqrt{3}R\,30°$-Ag and Si(111) $\sqrt{3} \times \sqrt{3}R\,30°$-Au.[23]

The sample was a (111) platelet of n-type Ge (30–40 Ω cm) with dimensions $1.5 \times 0.5 \times 0.05$ cm^3. It was held
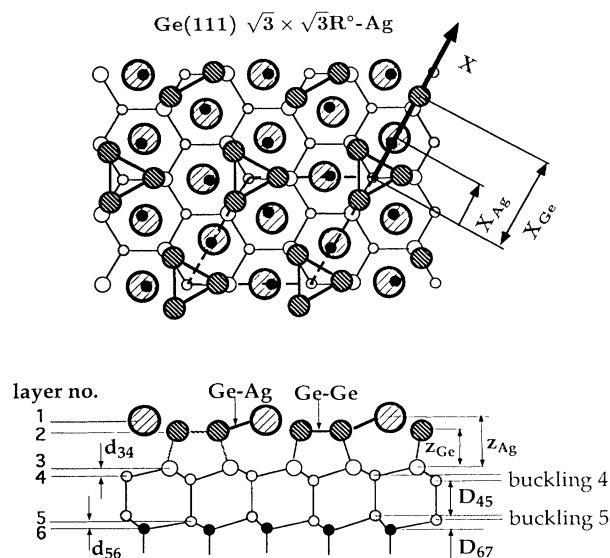
FIG. 1. The HCT model for Ge(111) $\sqrt{3} \times \sqrt{3}R\,30°$-Ag, showing distortions from bulk positions down to the sixth atomic layer. The biggest circles denote Ag atoms, Ge atoms in layers 2, 3, and 4 are denoted by circles with decreasing radii. The solid circles denote sixth-layer atoms.

    <u>49</u>   13 483

in place on a molybdenum plate by means of thin (0.025) mm) molybdenum tabs, and attached to a goniometer which allowed translations along three perpendicular axes, rotations around two of the axes, tilt about the third axis, and heating of the sample to about 1400 °C. The base pressure in the experimental chamber, after bakeout and outgassing of filaments, was typically $2.0E-10$ Torr. The sample surface was cleaned *in situ* with several cycles of Ar-ion bombardments ($5.0E-5$ Torr, 375 V, 2 μA) followed by 10-min anneals at about 800 °C. LEED showed a good Ge(111) $c(2\times8)$ pattern. Auger-electron spectroscopy (AES) (measured with the LEED optics as a retarding-field analyzer) revealed no carbon, oxygen, or other impurities above the noise level.

Silver atoms were deposited on the clean sample surface from an Ag source consisting of a fine (0.175 mm diameter) Ag wire firmly wound on a tungsten basket which was heated resistively. The surface coverage of Ag was determined from the ratio R of the (doubly differentiated) AES signals of Ag and Ge:

$$R = [I_{Ag(352)}/I_{Ge(52)}]$$

$$\times [\{1-\exp(-d/\lambda_{Ag})\}/\exp(-d/\lambda_{Ge})] , \quad (1)$$

where the AES signals of the semi-infinite materials $I_{Ag(352)}$ and $I_{Ge(52)}$ were determined to be 36.5 and 24.2, respectively. The inelastic mean free paths λ were taken to be 8.6 and 3.7 Å for Ag and Ge, respectively.[24] Corrections were applied to account for the angle subtended by the LEED-optics detector. The thickness of the Ag layer, determined in Å with the above formula, was converted to layer equivalents (LE's) by assuming a thickness of 2.89 Å for each Ag layer.

The LEED patterns observed upon deposition of Ag on the clean Ge(111) surface are described as follows. Deposition of 1–7 LE's of Ag on the clean substrate kept at room temperature gradually blurred the $c(2\times8)$ pattern and produced a mixture of Ag(111) 1×1 and Ge(111) 1×1 patterns. Subsequent anneals at about 300 °C for 10 min reduced the Ag coverage typically to 0.8 LE and produced a $\sqrt{3}\times\sqrt{3}R30°$ pattern. This pattern persisted (with the same diffracted intensities) even after increase of the annealing time or after increase of the annealing temperature up to 500 °C, although the measured Ag coverage was then reduced to 0.5 LE. The $\sqrt{3}\times\sqrt{3}R30°$ structure was found to be very stable even after leaving the sample in the experimental chamber at base pressure for several days. Anneals at 600–650 °C created a mixture of 4×1 and $\sqrt{3}\times\sqrt{3}R30°$ patterns, while anneals at higher temperatures removed all remaining Ag from the surface region and restored a clean, well-ordered $c(2\times8)$ structure.

LEED IV spectra were measured from the $\sqrt{3}\times\sqrt{3}R30°$ surface with a computer-controlled video-acquisition system.[25] The spectra were collected several times after renewed surface preparation and were found to be well reproducible. The IV spectra were taken at normal incidence so the LEED pattern showed C_{3v} symmetry. A total of 36 fractional-order and 24 integral-order spectra were collected, from which nine and seven inequivalent fractional- and integral-order spectra, re-

spectively, were obtained by averaging symmetrically equivalent beams. The spectra were then normalized to constant incident electron current, corrected for background, and smoothed by using Gaussian filters.

The dynamical LEED intensity calculations were performed using real and reciprocal space-symmetrized codes.[26–32] The full multiple-scattering calculations employed up to ten spin-averaged phase shifts, and the atomic scattering matrices were corrected for the effect of dynamical and static disorders using a constant Debye temperature of 450 K for Ge, and a variable Debye temperature for Au. An imaginary inner potential of 4 eV was used to represent the effect of inelastic scattering. The agreement between experimental and theoretical IV data was quantified by the Pendry r factor.[33] The LEED analysis described here was restricted to discriminating between the HCT and CHCT models only. This restriction represented no crucial loss of generality because an extensive structural search had been carried out previously for Ag and Au reconstructions on Si(111). The structures of Ag, Au on Ge(111), and Si(111) are similar in many respects.

The experimental IV curves of Ge(111) $\sqrt{3}\times\sqrt{3}R30°$-Ag were analyzed in two stages: First, a wide-range grid search was carried out.[26–30] The structural parameters were varied in steps 0.05–0.1 and 0.1–0.2 Å for the vertical and lateral displacements, respectively. In this search, all significant atomic positions were varied independently over a large volume of parameter space. Several local r-factor minima were found which served as starting geometries for structural refinement. In the refinement step, an extended version of a nonlinear least-squares optimization procedure[30–32,34] with respect to the Y function[33] was applied. Up to 11 structural parameters as well as the Debye temperature of Ag and the constant part of the real inner potential were varied simultaneously.

TABLE I. Atomic coordinates in Å for Ge(111) $\sqrt{3}\times\sqrt{3}R30°$-Ag compared to Si(111) $\sqrt{3}\times\sqrt{3}R30°$-Ag taken from Ref. 10. S represents the semiconductor (Si, Ge) atoms, the layer index (see Fig. 1) is in parentheses. Ag-Ag and S(2)-S(2) denote nearest-neighbor distances in an atomic plane. The x coordinate and other symbols refer to those shown in Fig. 1.

	Ag/Ge	Ag/Si
X_{Ag}	2.93±0.06	2.80±0.08
$X_{S(2)}$	5.35±0.06	5.21±0.08
$X_{S(3)}$	4.78±0.01	4.50±0.10
Ag-Ag	3.58±0.06	3.45±0.10
$S(2)$-$S(2)$	2.72±0.08	2.49±0.10
Z_{Ag}	3.13±0.03	3.00±0.03
Z_S	2.43±0.03	2.31±0.03
Z_{Ag}-Z_S	0.70±0.04	0.69±0.06
buckling 4	0.33±0.04	0.20±0.05
buckling 5	0.19±0.05	0.14±0.07
D_{45}	2.20±0.03	2.31±0.03
D_{67}	2.46±0.05	2.21±0.05
d_{34}	0.73±0.03	0.68±0.03
d_{56}	0.67±0.05	0.71±0.05

Our LEED structure resulted in a best r factor for the HCT model of 0.40, while the best r factor for the CHCT model was significantly worse, namely 0.76. Based on these r factors, the CHCT model was definitely ruled out. The optimal HCT model has the following structural characteristics: The Ag atoms replace the top Ge layer [of the bulk-truncated Ge(111) surface]. They are shifted laterally from bulk sites by 0.62 Å. A major feature of the model is that the Ge atoms in the second layer are displaced by 0.74 Å to form trimers centered above fourth-layer atoms. The formation of Ge trimers satisfy two of the three dangling bonds, while the remaining dangling bond is used to bond with an Ag atom. The formation of Ge trimers greatly distorts the substrate lattice, and large relaxations down to the sixth atomic layer are induced. Vertical displacements of Ge atoms result in buckled fourth and fifth layers with thicknesses of 0.33 and 0.19 Å, respectively. A lateral displacement of 0.17 Å in the third layer is also present (Table I: $X_{Ge(3)}=4.78\pm0.1$ Å). By symmetry, lateral displacements in the fourth and fifth layers are not allowed. The

top interlayer spacing between Ag and Ge is 0.70 Å. These results are summarized in Table I and compared with those of Si(111) $\sqrt{3}$-Ag. Atoms in the seventh and deeper layers are held at bulk sites. The nonstructural parameters for the optimal model are 4 eV for the real part of the inner potential, and 90 K for the Debye temperature. The small Ag Debye temperature is attributed to enhanced movements of Ag atoms around their equilibrium positions. The agreement of IV spectra between experiment and theory for the optimal structure is illustrated in Figs. 2 and 3.

There is further evidence to corroborate the HCT model for the Ge(111) $\sqrt{3}$-Ag system. Fan and Ignatiev[35] have observed that the LEED IV spectra for the $\sqrt{3}$ structures of Ag/Ge(111), Li/Ge(111), and a clean Ge(111) metastable reconstruction are very similar. The same phenomenon is observed on Si(111).[36] In a recent LEED analysis,[10] this similarity in IV spectra is explained by the presence in these systems of the same "scattering block" comprised of second-layer Si trimers and deeper-layer atoms. The weak influence on the IV
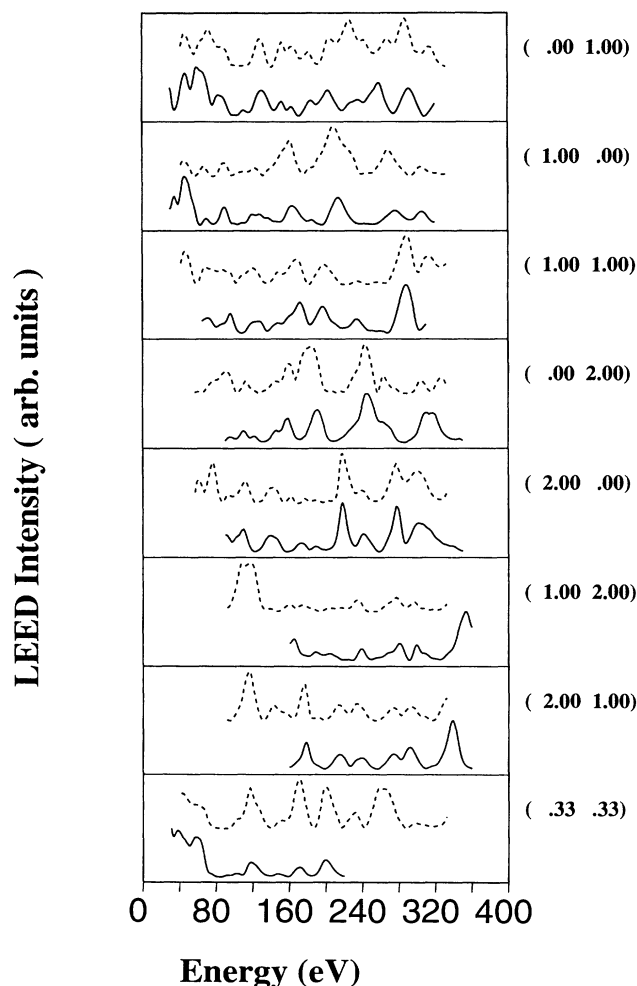
FIG. 2. Comparison of IV spectra between experiment (solid lines) and theory (dashed lines) for the optimal HCT model for seven integral-order beams and one fractional-order beam.
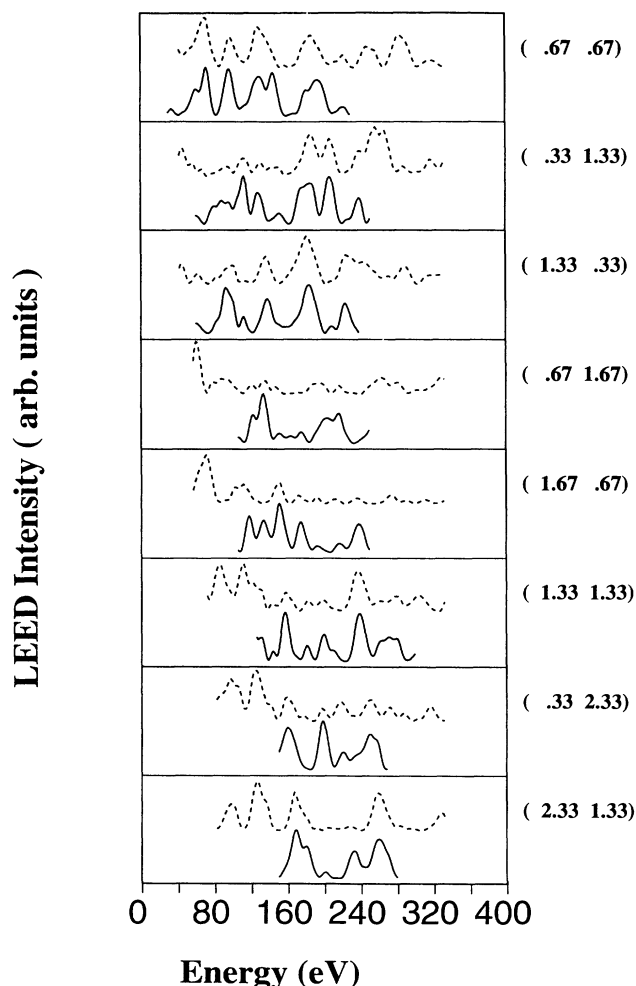
FIG. 3. Comparison of IV spectra between experiment (solid lines) and theory (dashed lines) for the optimal HCT model for eight fractional-order beams.

TABLE II. Comparison of the $(\sqrt{3} \times \sqrt{3})\, R\,30°$ reconstruction formed by Ag or Au on Si(111) or Ge(111).

System: $(\sqrt{3} \times \sqrt{3})\, R\,30°$	Metal-metal n-n distance	Bond lengths: substrate trimer	Model	Reference & method
Ag/Si(111)	3.45±0.10 Å	2.49±0.10 Å	HCT	10 LEED
Au/Si(111)	2.81±0.06 Å		CHCT	20 LEED
Ag/Ge(111)	3.58±0.06 Å	2.72±0.08 Å	HCT	this study
Au/Ge(111)	2.81±0.02 Å		CHCT	21 XRD

curves of metal atoms at the surface layer is due to their location at "open" sites, i.e., the metal atoms are located above sixth-layer atoms. Also, in the clean $\sqrt{3} \times \sqrt{3}$ reconstructions of Si(111) and Ge(111), no ordered metal atoms are present. Therefore, the common scattering block must consist solely of substrate atoms. Applying these findings to the Ge(111) $\sqrt{3} \times \sqrt{3}R\,30°$-Ag system, we conclude that, again, the Ge trimer is the common scattering block and that the metal atoms (either Ag or Li) are located at "open" sites. A corollary of this result is that the atomic configuration of Ge(111) $\sqrt{3} \times \sqrt{3}R\,30°$-Li is also the HCT model, although the precise atomic coordinates are not determined because the available data base is small. Another interesting corollary is that Ge(111) $\sqrt{3} \times \sqrt{3}R\,30°$-Au should have very different IV spectra from those of Ge(111) $\sqrt{3} \times \sqrt{3}R\,30°$-Ag. The HCT model for Ge(111) $\sqrt{3} \times \sqrt{3}R\,30°$-Ag received further support in a recent STM investigation:[37] Hammar et al.[37] observed a sixfold honeycomb image, in close conformity with the image of Si(111) $\sqrt{3} \times \sqrt{3}R\,30°$-Ag, but differs from that of Si(111) $\sqrt{3} \times \sqrt{3}R\,30°$-Au.[15]

With the HCT model found for Ge(111) $\sqrt{3} \times \sqrt{3}R\,30°$-Ag, a "simple" picture evolves for the adsorption of Ag and Au on Si(111) and Ge(111) (see Table II). According to this picture, the Si-Si and Ge-Ge in-

teractions dominate in the Ag-$\sqrt{3}$ interface systems. It is the substrate trimerization that drives the systems into a HCT configuration. With the Au-$\sqrt{3}$ interface systems, the opposite is true: The Au-Au interaction dominates and the metal trimerization is the driving force that causes the CHCT model to form on Si(111) and Ge(111). This picture also explains why the Au-Au bond lengths in the $\sqrt{3} \times \sqrt{3}R\,30°$ reconstructions of Si(111) and Ge(111) are almost identical.

In summary, we have carried out a quantitative LEED spectra analysis of the Ge(111) $\sqrt{3} \times \sqrt{3}R\,30°$-Ag system. The HCT model is favored over the CHCT model. This structural result provides a consistent picture for Ag and Au adsorption on the Si(111) and Ge(111) surfaces, in terms of metal-metal and semiconductor-semiconductor bond strengths at the interface.

ACKNOWLEDGMENTS

*Present address: Fritz Haber Institut der Max Planck Gesellschaft, Faradayweg 4-6, D-14195 Berlin, Germany.

[1] G. Le Lay, Surf. Sci. 132, 169 (1983).

[2] E. Vlieg, A. W. van der Gon, J. F. van der Veen, J. E. MacDonald, and C. Norris, Surf. Sci. 209, 100 (1989).

[3] T. Takahashi, S. Nakatani, N. Okamoto, T. Ichikawa, and S. Kikuta, Jpn. J. Appl. Phys. 27, L753 (1988).

[4] A. Ichimiya, S. Kohmoto, T. Fujii, and Y. Horio, Appl. Surf. Sci. 41/42, 82 (1989).

[5] E. Vlieg, E. Fontes, and J. R. Patel, Phys. Rev. B 43, 7185 (1991).

[6] Y. G. Ding, C. T. Chan, and K. M. Ho, Phys. Rev. Lett. 67, 1454 (1991).

[7] M. Katayama, R. S. Williams, M. Kato, E. Nomura, and M. Aono, Phys. Rev. Lett. 66, 2762 (1991).

[8] Y. Tanishiro, K. Takayanagi, and K. Yagi, Surf. Sci. 258, L687 (1991).

[9] K. J. Wan, X. F. Lin, and J. Nogami, Phys. Rev. B 45, 9509 (1991).

[10] H. Over, H. Huang, S. Y. Tong, W. C. Fan, and A. Ignatiev, Phys. Rev. B 48, 15 353 (1993).

[11] R. J. Wilson and S. Chiang, Phys. Rev. Lett. 58, 369 (1987).

[12] E. J. Van Loenen, J. E. Demuth, R. J. Tromp, and R. J. Hamers, Phys. Rev. Lett. 58, 373 (1987).

[13] R. J. Wilson and S. Chiang, Phys. Rev. Lett. 59, 2329 (1987).

[14] A. Ph. Dumas, G. Humbert, P. Mathieu, C. Mathiez, R. Mouttert, F. Roland, F. Salvan, and F. Thibaudau, J. Vac. Sci. Technol. A 6, 517 (1988).

[15] J. Nogammi, A. A. Baski, and C. F. Quate, Phys. Rev. Lett. 65, 1611 (1990).

[16] D. Dornisch, W. Moritz, H. Schulz, R. Feidenhans'l, M. Neilsen, F. Grey, and R. L. Jonson, Phys. Rev. B 44, 11 221 (1991).

[17] K. Oura, M. Katayama, F. Shoji, and T. Hanawa, Phys. Rev. Lett. 55, 1486 (1985).

[18] M. Chester and T. Gustafsson, Surf. Sci. 256, 135 (1991).

[19] Y. G. Ding, C. T. Chan, and K. M. Ho, Surf. Sci. Lett. 275, L691 (1992).

[20] J. Quinn, F. Jona, and P. M. Marcus, Phys. Rev. B 46, 7288 (1992).

[21] P. B. Howes, C. Norris, M. S. Finney, E. Vlieg, and R. G. van Silfhout, Phys. Rev. B 48, 1632 (1993).

[22] B. J. Knapp and J. G. Tobin, Phys. Rev. B 37, 8656 (1988).

[23] D. Dornisch, W. Moritz, H. Schulz, R. Feidenhans'l, M. Niel-

sen, G. Grey, R. L. Jonson, and G. Le Lay, Surf. Sci. **274**, 215 (1992).

[24]M. P. Seah and W. A. Dench, Surf. Interf. Anal. **1**, 2 (1979).

[25]F. Jona, J. A. Strozier, and P. M. Marcus, in *The Structure of Surface*, edited by M. A. Van Hove and S. Y. Tong (Springer-Verlag, Berlin, 1985), p. 92.

[26]M. A. Van Hove and S. Y. Tong, *Surface Crystallography by LEED* (Springer-Verlag, Berlin, 1979).

[27]M. A. Van Hove, W. H. Weinberg, and C. M. Chan, *Low Energy Electron Diffraction* (Springer-Verlag, Berlin, 1986).

[28]H. Huang, S. Y. Tong, W. E. Packard, and M. B. Webb, Phys. Lett. A **130**, 166 (1988).

[29]S. Y. Tong, H. Huang, C. M. Wei, W. E. Packard, F. K. Men,

G. Glander, and M. B. Webb, J. Vac. Sci. Technol. A **6**, 615 (1988).

[30]W. Moritz, J. Phys. C **17**, 353 (1984).

[31]G. Kleinle and W. Moritz, G. Ertl, Surf. Sci. **238**, 119 (1990).

[32]H. Over, U. Ketterl, W. Moritz, and G. Ertl, Phys. Rev. B **46**, 15 438 (1992).

[33]J. Pendry, J. Phys. C **13**, 937 (1980).

[34]M. Gierer, H. Over, W. Moritz, and G. Ertl (unpublished).

[35]W. C. Fan and A. Ignatiev, Phys. Rev. B **40**, 5479 (1989).

[36]W. C. Fan, A. Ignatiev, H. Huang, and S. Y. Tong, Phys. Rev. Lett. **62**, 1516 (1989).

[37]M. Hammar, M. Gothelid, U. O. Karlsson, and S. A. Flodstrom, Phys. Rev. B **47**, 15 669 (1993).